Reversible Dimerization and Polymerization of a Janus Diradical To Produce Labile CC Bonds and Large Chromic Effects

Reversible Dimerization & Polymerization of a Janus Diradical Producing Labile CC Bonds and Giant Chromism

José L. Zafra[1], Lili Qiu[2], Naoyuki Yanai[3], Takamichi Mori[3,4], Masahiro Nakano[4], Miriam Peña Alvarez[5], Juan T. López Navarrete[1,a] Carlos J. Gómez-García[6], Miklos Kertesz[2], Kazuo Takimiya[3,4*] and Juan Casado[1*]

[1] Department of Physical Chemistry, Faculty of Sciences, CEI Andalucía Tech - University of Malaga, 29071 Malaga, Spain

[2] Department of Chemistry and Institute of Soft Matter, Georgetown University, 37th and O Streets, NW, Washington, D.C. 20057-1227, USA

[3] Department of Applied Chemistry, Graduate School of Engineering, Hiroshima University, Kagamiyama. Higashi-Hiroshima 739-8527 Japan

[4] Emergent Molecular Function Research Group, RIKEN Center for Emergent Matter Science (CEMS) 2-1 Hirosawa, Wako, Saitama, 351-0198, Japan

[5] Department of Physical Chemistry, Complutense University of Madrid, 28040 Madrid, Spain

[6] Instituto de Ciencia Molecular, Universidad de Valencia 46980 Paterna, Valencia, Spain.

*To whom all correspondence should be sent: E-mail: takimiya@riken.jp, casado@uma.es

Abstract. Conducting polymers can be synthesized via irreversible diradical monomer polymerization. A reversible version of this reaction mechanism consisting of the formation/dissociation of σ–dimers and σ–polymers from a stable quinonoidal diradical precursor is described. The reversible diradical-mediated reaction here is made by a quinoidal molecule which changes its structure to aromatic by forming weak and long intermolecular C-C single bonds, either in σ–dimers or σ–polymers. The reaction provokes a giant chromic effect of ≈ 2.5 eV from the blue quinonoidal precursor to the colorless σ–bonded aromatic aggregates. The opposite but complementary quinoidal and aromatic valence tautomeric structures provide the two Janus faces of the reactants and products that is at the origin of the observed giant chromism. A reaction mechanism is proposed which includes important entropic effects explaining the variety of final products starting with structurally very similar reactants. These unique reversible soft reactions, covering an unusual regime of weak covalent supramolecular bonding, represent a new way to generate adducts with potential applications in chromism and in material science by envisaging new molecular and polymeric materials forming novel soft matter phases.

Some important conducting polymers[1], i.e. poly(paraphenylene-vinylene)[2], are prepared via a diradical polymerization with monomers able to generate highly reactive quinonodimethane diradical intermediates.[3] The high reactivity of these diradicals provokes the formation of chemically "irreversible" strong inter-monomer C–C single bonds sustaining the polymer backbone (Scheme 1). The "reversible" version of this polymerization mechanism is the subject of this work. In contrast to the former, "reversible-made" polymers might broaden the material versatility since one can move back and forth in the monomer/polymer equilibrium by soft external physical and environmental stimuli.[4] The key aspect that differentiates the chemically "reversible" and "irreversible" paths is the stability of the diradical precursor. Therefore, a clear structure-property relationship should be established: more versatile molecular and polymeric "reversible-made" multifunctional materials should be based on highly stable diradical precursors.[5]

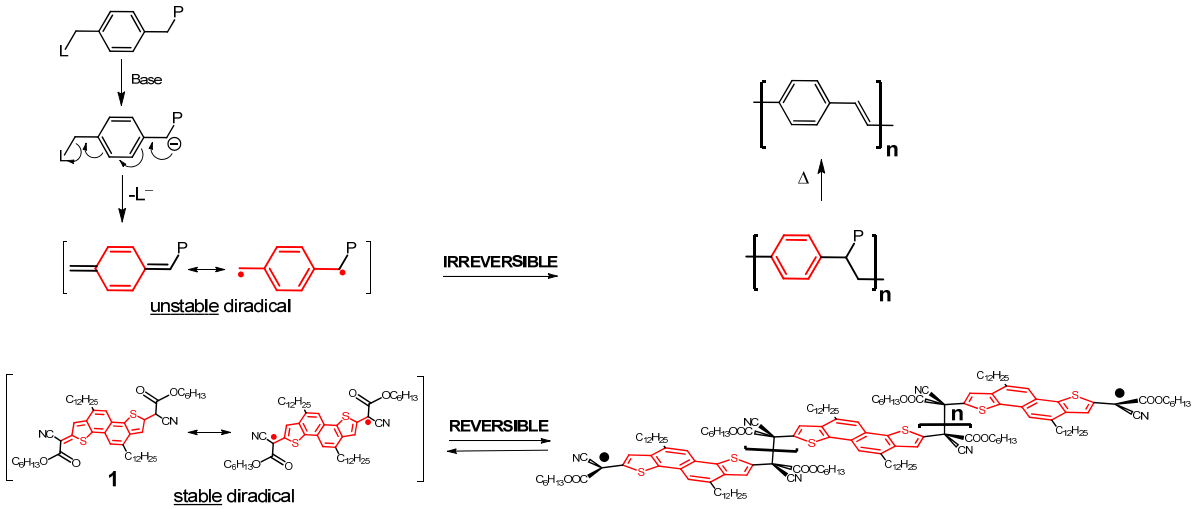

Scheme 1 | Diradical polymerization mechanisms. Top, polymerization of poly-paraphenylenevinylene. Bottom, polymerization of **1** in this study.

Chromism,[6] a niche reserved for π-conjugated organic dyes, is a valuable property for functional materials,[7] and sometimes emerges as a manifestation of new underlying chemical phenomena. There are plenty of good examples of thermo- and electro-chromic conjugated polymers,[8] whereas, there are only a few cases based on neutral small molecules: for instance, neutral mono-radicals, such as imidazolyl (**im**)[9] and phenalenyl (**ph** and **phN**)[10] derivatives. Double-radical or diradicals based on the diphenalenyl (**dph**) cores[11,12] have been also shown to

promote chromism by the formation of staircase π–stacking oligomers (and π–stacking polymers) through co-facial bonding between the radicaloid centres *via* the so-called pancake bonding. [13] In the case of the tetrafluorobisimidazol quinonoidal compound (**dim**) the exchange between green and pale yellow colors is mediated by a photo-chemical diradical dimerization with double formation of C-N bonds.[14] See Scheme 2 for the chemical structures of these compounds.

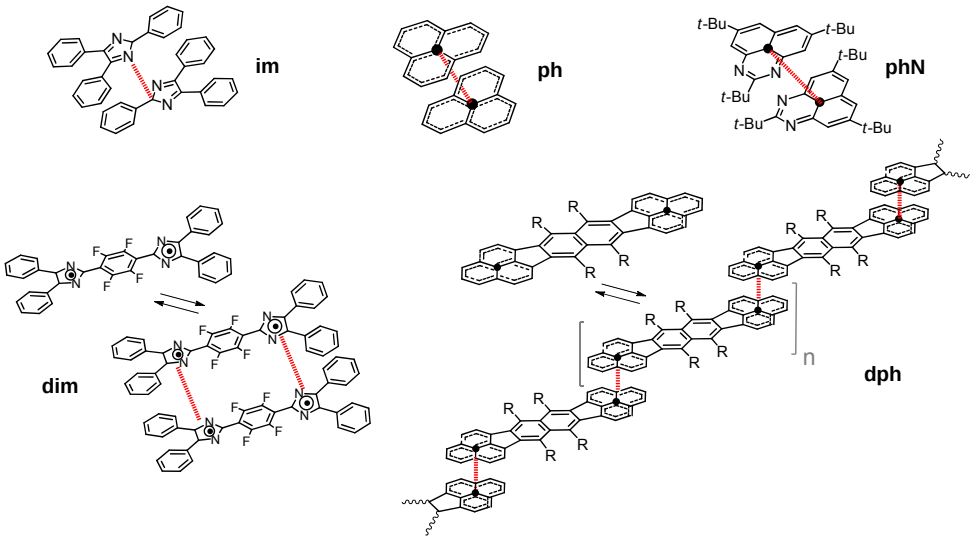

Scheme 2 | Polycyclic compounds forming σ–aggregates. Imidazolyl (**im**), phenalenyl (**ph** and **phN**), diphenalenyl (**dph**) and tetrafluorobisimidazol quinonoidal (**dim**) derivatives.

The mediation of unpaired electrons is common in all these cases. Radical centres are capable to promote either multicenter delocalized pancake π–bonds or localized σ–bonds, the latter giving rise to unusually long C-C bonds.[15,16] In fact, σ– and π–products represent two competitive routes along the intermolecular dimerization/polymerization reaction pathway as they feature two different minima in the energy path from reactants to products.[17,18] The result of the distinctive molecular reorganization after π– or σ–bonding provokes different chromism.

Recently, tetracyanoquinonoidal oligothiophenes (Scheme 3a) have been intensively studied.[19,20,21,22] For those with a small number of thiophenes, the ground electronic state has a singlet closed-shell quinonoidal structure, whereas in the medium-large members, the quinonoidal structure converts into a singlet open-shell diradical with aromatic structure (Scheme 3a). [19,20] Very useful functions have

been described for such quinonoidal oligothiophenes such as magnetic switching,[23] electrochromism[24] and very recently singlet exciton fission[25,26] for photovoltaics.

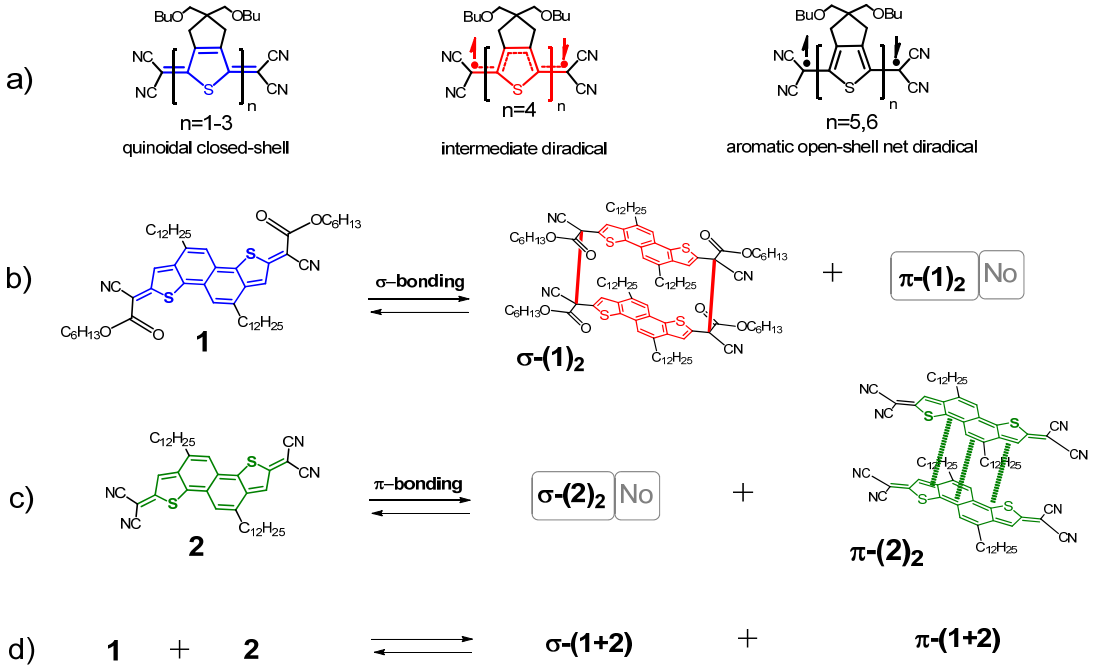

Scheme 3 | Quinonoidal oligothiophenes and molecules under study. a) Tetracyano quinonoidal oligothiophenes from a monomer to a hexamer displaying the diradical character with size. Dimerization reactions of **1** (b) and **2 (**c**).** (d) σ– and π–dimerization of **1**+**2** (mixed dimers).

We present a new outstanding behavior of these heteroquinoidal molecules: reversible diradical σ–dimerization/σ–polymerization of **1** (Scheme 1 and 3b) triggered by "soft" stimuli (concentration, temperature and pressure). The reaction is accompanied by a 2.5 eV chromic effect which originates from the transformation of its quinoidal core in the monomer into an aromatic electronic structure in the σ–dimer or σ–polymer. σ–Dimerization of **1**, σ–(**1**)$_2$, takes place in dilute solutions. However, when combined with another very similar quinoidal molecule, **2,** unusual mixed σ– and π–dimers, σ–(**1**+**2**) and π–(**1**+**2**), are observed (Scheme 3b/d). Conversely, **2** only forms π–dimers, π–(**2**)$_2$ (Scheme 3c). **1**, furthermore, in concentrated solutions or by forming solid films by drop-casting results in the same phenomena of reversible chromisms which we ascribe to the formation of σ–oligomers or σ–polymers. We obtain further insights into these unusual molecular associations by observing heat and pressure effects in the solid

state. Remarkably, these association reactions are completely reversible and provide new molecular platforms for applications in materials science.

Results and Discussion

σ–Dimerization and σ–polymerization of 1. We have prepared the new quinoidal compound **1** with two thiophenes fused with a naphthalene and having cyano-alkyloxycarbonyl-methylene functionalities at the outermost positions (see Scheme S1 for synthesis). In comparison with its dicyano-methylene counterpart **2**, the molecular optical properties are barely modified (Figure 1a).[27,28] In fact, both **1** (λ_{max} = 635 nm) and **2** (λ_{max} = 625 nm) display very intense blue color in solution.

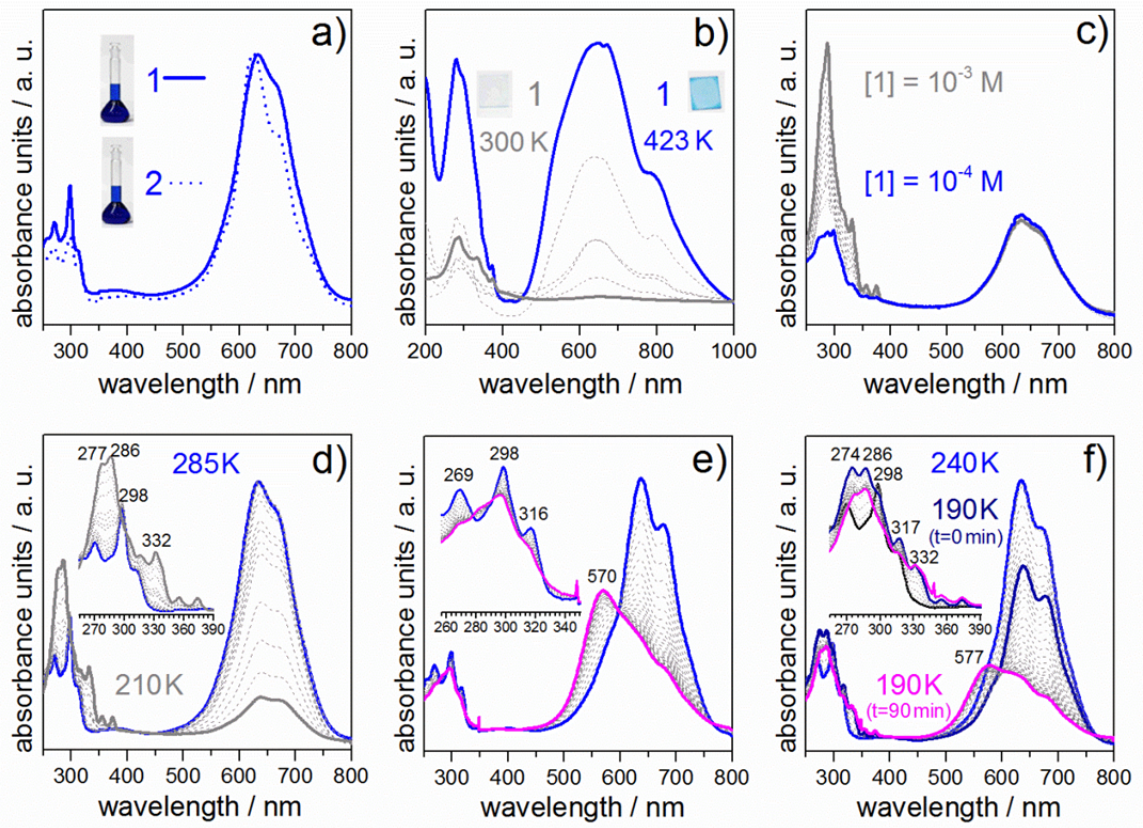

Figure 1 | UV-Vis spectrophotometric characterization of the dimerizations. a) **1** and **2** at 300 K in dilute (10^{-5} M) solutions of dichloromethane (as quinononoidal monomers); b) **1** as solid drop-cast thin film at 300 K (grey solid line) and after heating at 423 K for 90 minutes (blue solid line); c) evolution of the spectrum of a 10^{-4} M solution of **1** at room temperature (blue solid line) in dichloromethane with the increase of the concentration up to 10^{-3} M (grey solid line). d) 10^{-5} M dilute solution of **1** in dichloromethane by cooling; e) 10^{-5} M dilute solution of **2** in dichloromethane by cooling from 285 K (blue line) to 190 K (pink line); f) 10^{-5} M equimolar solution of **1**+**2** by cooling from 300 K to 190 K and then waiting for 90 minutes at 190 K.

The first unexpected result is that when **1** was deposited as a thin solid film by drop-casting from solution, the resulting film became completely colorless (see Movie S1). After re-dissolution of the thin film of **1**, the blue color was fully recovered. Figure 1b displays the UV-Vis absorption spectra of the transparent drop-cast thin film of **1** which shows new bands around 270-330 nm. Moreover, we have reproduced the same chromic phenomenon starting with a dilute 10^{-5} M solution of **1** in dichloromethane by lowering the temperature (Figure 1c/d and Movie S2). With cooling, we observe the growing of a high energy band with peaks centered at 270-330 nm which are very similar to those of the drop-cast solid film. The emergence of these new bands was accompanied by the disappearance of the main absorption at 635 nm (isosbestic point at 450 nm). When the frozen colorless solution was heated back to room temperature, the original blue band was fully re-established (Figure 1d). The thermal cycle can be repeated multiple times and conducted in methylcyclohexane and in methyltetrahydrofuran yielding identical observations. The thermal treatment was also applied to the colorless thin film (Figure 1b), which showed that heating from room temperature allowed a progressive recovery of the visible blue band at temperatures higher than 400 K. At room temperature, similar UV-Vis spectral features are observed starting with a dilute solution of **1** by increasing the concentration (Figure 1c): at high concentrations, the bands at 270-330 nm clearly arise again whereas the blue band decreases (without full interconversion). Compound **2** does not show any of these transformations (Figure S1).

Temperature dependent experiments in the dilute solution allowed us to derive thermodynamic parameters of the reaction. Assuming a dimerization process, we have obtained the equilibrium constant K(T) at several temperatures and by means of a van´t Hoff plot (K(T)-1/T) the variation of dimerization reaction enthalpy (ΔH^o) is obtained (Figure S2) with values of −14.81 kcal/mol (CH_2Cl_2), −10.59 kcal/mol (C_6H_{12}) and −8.57 kcal/mol in (Me-THF). In addition the variation of the entropy of the dimerization reaction, ΔS^o, is calculated to be: −0.048 kcal/K.mol in dichloromethane, −0.065 kcal/K.mol in methylcyclohexane and −0.058 kcal/K.mol

in methyl tetrahydrofurane at 273 K. These data indicate that the exothermic character provides the driving force for the reaction.

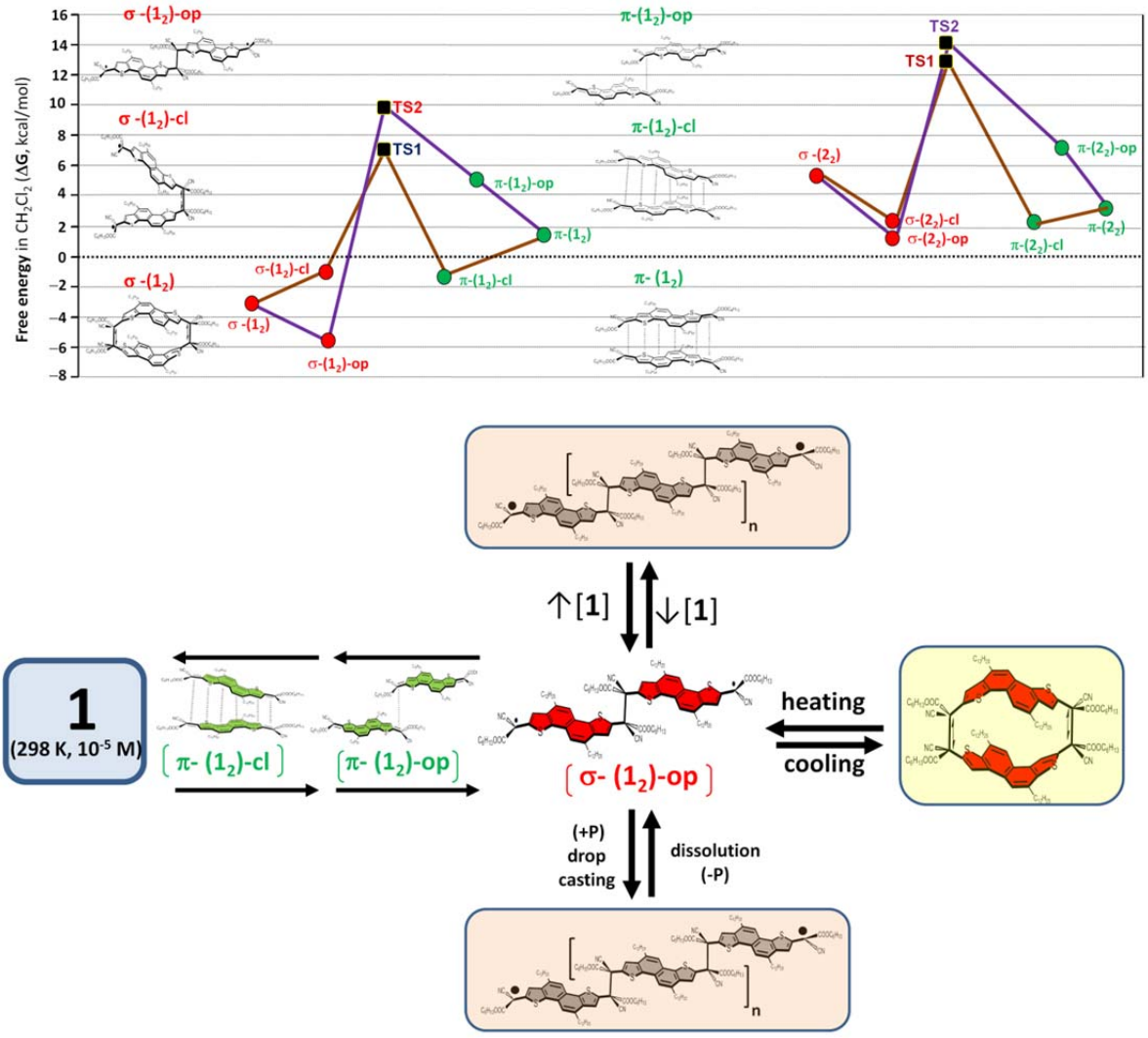

Figure 2 | Free energy calculations along the dimerization reaction. Top: Relative Gibbs free energies ($\Delta G=G_{dimer}-2G_{monomer}$) of each dimerization reaction of compound **1** (left) and **2** (right) calculated in CH_2Cl_2. Lines are provided to guide the eye. All structures are local minima except the transition structures. Chemical structures are drawn from the optimized geometries for **1**, structures for **2** are similar and are not shown. TS (black squares) indicate the transition structures between the σ- and π-sides according to either the closed path (maroon line, TS1) or through an open route (purple line, TS2). See the ESI file for detailed information of these calculations. Bottom: equilibria for σ–dimerizations and σ–polymerizations starting from π–dimerizations.

The energetics of the dimerizations from quantum chemical calculations are summarized in Figure 2 [29,30,31] (see Figures S3-S11 and Tables S1-S3). For the dimeric stacking configurations, we considered the *syn*- and *anti*-orientations with

respect to the positions of the sulphur atoms, with the *anti* being more stable except where indicated otherwise. We address two major *anti* electronic states, σ– and π–dimers, for which several conformations have been modeled, namely, open (i.e., **σ–(1_2)-op** or **π–(1_2)-op**) with only one connection between the two monomers, corresponding to the most extended conformation; fully closed with face-to-face coupling [i.e., **σ–(1_2)** with two σ–bonding sites or **π–(1_2)** with pancake bonding], and closed (i.e., **σ–(1_2)-cl** or **π–(1_2)-cl**) which is intermediate between the two former conformers (see Figure 2). In addition, transition states have been calculated between the σ and π sides for both **1** and **2**. The relative Gibbs free energies (ΔG, in Figure 2 and Table S3) have been calculated for each dimerization reaction from the monomer reactants and are always negative for the formation of σ–dimers of **1** pointing out to the spontaneity of these σ–dimerizations. Among these, the formation of σ–**(1_2)-op** is the most favorable reaction which drains the formation of other σ–dimers and is pivotal for the formation of σ–polymers (Figure 2). This is in contrast to the endergonic character of the π–dimerizations of **1** (except for **π–(1_2)-cl**). For compound **2**, the formation of σ–and π–dimers is computed to be endergonic at 298 K, however, one would expect that a decrease of the temperature would promote their formation (exothermic reactions). The free energy barriers towards the transition state for the σ↔π interconversion for **1** and **2** have been also evaluated and found that the smaller one is for the conversion from **π–(1_2)-cl** to **σ–(1_2)-op**, thus the solely stable π–dimer of **1** is more labile towards the conversion to the σ-bonded isomers. This reaction from π– to σ–dimers of **1** can go through two different mechanisms: a open or step-by-step route which first breaks the symmetry of the starting π–dimer (π–(**1_2**)) by forming a singly π–bonded diradical (**π–(1_2)-cl**) and then through TS1 (Figure S10) converts to the equivalent **σ–**(**1_2**)-cl (maroon line in Figure 2); and a concerted path which maintains the symmetry between the fragments during the reaction (purple line in Figure 2 through TS2, Figure S10); Although the transition barrier through TS1 is smaller than for TS2 both mechanism might be operative for the permanent fueling of σ–dimers. What is important is that diimerizations of **1** always forms first the labile

π–dimers which then evolve into σ– through one or another path. For **2**, these barriers are larger indicating that once π–dimers are formed at low temperature they would be more persistent.

Calculations for **1** and **2** monomers show significant diradical character (Table S1). Interestingly, this diradical character is enhanced and modulated by intermolecular interactions along the dimerization reaction coordinate giving rise to biradical dimer species, such as **σ-(1)$_2$–op**, and starting from this producing closed-shell cyclophane dimers such as **σ-(1$_2$).** For instance, the optimized geometry of monomer **1** displays a π–spin density of –0.4 e on the C atoms connecting the sp^2 carbons adjacent to the CN groups (Table S1-S2) which in **σ-(1$_2$)** are consumed in the formation of long highly strained C-C single σ-bonds with computed lengths of 1.676 Å (Figure S4).[32] In **σ-(1$_2$)-op** only one strained bond (1.623 Å, Figure S6) is formed leaving two unpaired electrons at the extremities. The structures of **σ-(1$_2$)** and **σ-(1$_2$)-op** feature aromatic substructures for the naphthalene and thiophene groups. For **σ-(1$_2$)** this central aromatic core is slightly bulging out (Figure S4) in order to minimize steric repulsions. TD-DFT excited state calculations[33] for **1** and **2** and their dimers show an excellent agreement with experiments in Figure 1 confirming that in the case of **1** the dominant final dimer product is **σ-(1$_2$)**, while for **2** the major dimer species is trapped as **π-(2$_2$)** (Table 1 and Figure S12).

Table 1 | Experimental and theoretical excitations energies. Absorption maxima and computed TDDFT/UM05-2x/6-31G(d,p) excitation energies for the most relevant bands of the dimers detected experimentally (in nm). Computed data refer to the more stable *anti* configuration except where so noted.

	1	**σ-(1$_2$)**	**σ-(1+2)**	**2**	**π-(2$_2$)**	**π-(1+2)**
experiment	635	277, 286	274, 287	625	570	577
computation	649	272, 292	239, 246[a]	663	587	582

[a] The *syn* dimer is the most stable configuration in this case.

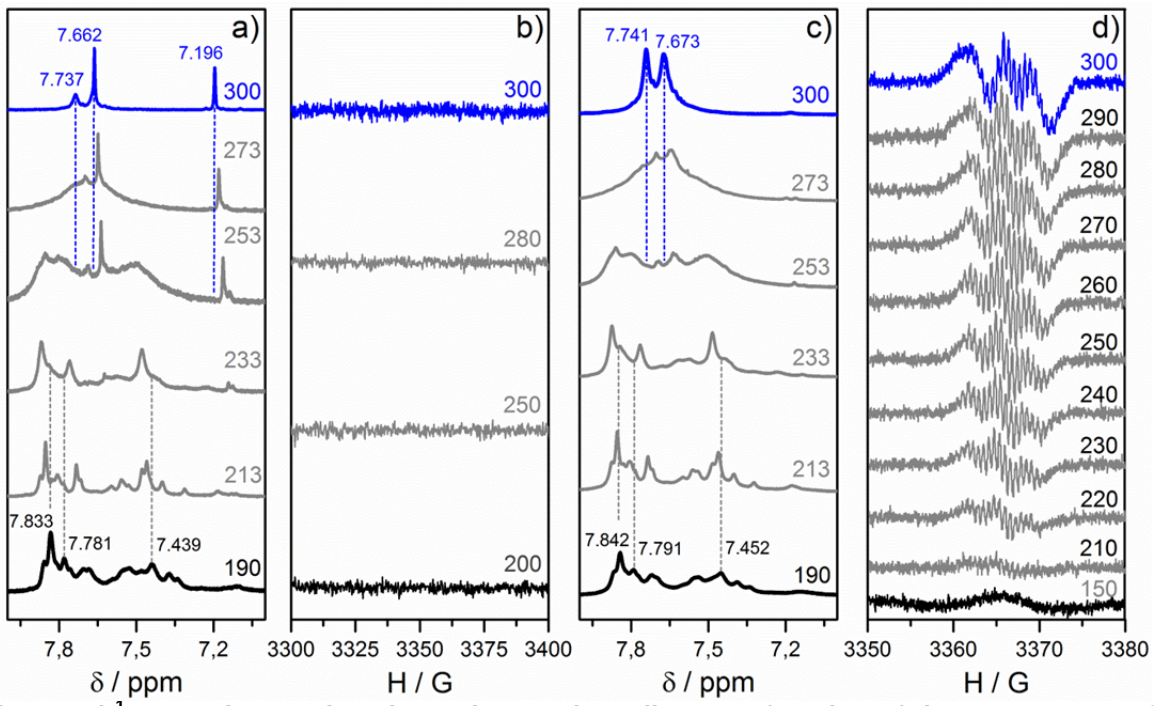

Figure 3 | ^{1}H NMR in CD_2Cl_2 and EPR in CH_2Cl_2 studies as a function of the temperature. a) and b) are for a 10^{-5} M dilute solution of **1** and c) and d) for a concentrated solution of **1**. Blue lines are for the spectra at high temperature and grey line spectra for those at low temperature.

Temperature dependent ^{1}H NMR data of **1** in a dilute solution are shown in Figure 3a. At room temperature two main peaks are assigned to the two different protons of the thiophene (δ=7.19 ppm) and of the naphthalene cores (δ=7.66 ppm) featuring a quinoidal structure (monomer **1**). These signals progressively disappear on cooling giving rise to multiple signals mainly placed down-field relative to those of the monomer in line with the formation of the aromatic structures (Figure S13). On the other hand, the same dilute solution of **1** was studied by EPR which does not give any resolvable signal at any temperature (Figure 3b and Figure S14).

The ^{1}H NMR spectrum of the 10^{-3} M concentrated solution of **1** at room temperature is shown in Figure 3c, which is also characterized by two peaks similarly placed down-field relative to those of the dilute solution of **1** supporting the formation under these conditions of another pseudo-aromatic structure. When this concentrated solution is analyzed by EPR spectroscopy, in contrast to the dilute regime, the room temperature spectrum shows a well resolved band with up to 15

lines (Figure 3d) resulting from the hyperfine coupling of unpaired electrons with the thiophene and naphthalene H and N atoms (Figure S15 and Table S4). The intensity of this signal progressively decreases as the temperature is lowered down to ca. 200 K. This ^{1}H NMR/EPR behavior is consistent with the formation of the EPR active and aromatic species such as **σ-(1_2)-op** in the concentrated solution which, on cooling, can trap monomers by the two termini giving way to a propagation step towards the formation of long σ–oligomers or σ–polymers with the concomitant decrease of the EPR signal. In the dilute solution, **σ-(1_2)-op** might be also initially formed but it cannot react inter-molecularly, however it can react intra-molecularly by reorienting the fragments to make a second strained single CC bond in **σ-(1_2)**, which is an EPR silent aromatic cyclophane species.

The EPR study has been also carried out for the drop-cast thin solid of **1**. At room temperature, it gives rise to a well resolved doublet EPR signal[34] (Figure S16 and S17) which increases its intensity by heating up to 400 K and then progressively disappears when cooling down to ca. 280 K in correspondence with the formation of a σ–polymer of **1** at room temperature which is destroyed by heating and then recovered by cooling. Again these EPR cycles are reversible (Figure S18). This colorless thin solid film has been also analyzed by means of FTMS ICP mass spectrometry (Figure S19) and found the strongest peak due to the molecular weight at 909.56659 followed by secondary peaks of lower intensity at 1820.13428 and at 2731.70386 which correspond to twice and three times the molecular peak. This is a direct evidence of the formation of oligomers of **1** in the drop-cast thin solid film likely resulting from the fragmentation of the σ–polymer. X-ray diffraction measurements on this drop-cast thin solid film in Figure S20 display a broad unresolved band clearly indicative of an amorphous phase. Therefore, diradical **σ-(1_2)-op** is a key intermediate which is formed first from the monomers through the π–dimer intermediates. This, in dilute solutions, allows the formation of a double **σ-(1_2)** cyclophane dimer by intramolecular long C-C bond formation, whereas in highly concentrated solutions or during the formation of the drop-cast thin film by

evaporation, **σ-(1_2)-op** represents the first step of the propagation mechanism of the oligomerization/polymerization reaction.

π–Dimerization of 2. A cooling process identical to that of **1** was carried out for a dilute solution of **2** and followed by UV-Vis absorption (Figure 1f). At low temperatures, the main absorption band of the monomer develops a single new band at 570 nm which gives a rosy-blush color to the cold solution (no bands around 300 nm are observed). This 570 nm band at low temperatures of **2** is predicted by TDDFT calculations at 587 nm for its π–dimer, **π-(2_2)** Table 1 and Figure S21) with no traces in the spectra of the formation of **σ-(2_2)**. In spite of the structural similarity, while **1** only forms **σ-(1_2)**, **2** only forms **π-(2_2)**, an experimental behavior accounted by the exoergic character of **1** ↔ **σ-(1_2)** (oppositely, **2** ↔ **σ-(2_2)** is endergonic) whereas **2** ↔**π-(2_2)** are quickly formed and kinetically trapped by large isomerizations barriers along the dimerization reaction paths. The needed assessment of free energies to account for the reaction mechanism reveals the impact of entropic control in the reactions in **1** and **2**. It seems that the occurrence in **1** of more soft vibrational modes might be at the origin of the different entropy contributions (i.e., out-of-plane modes are more feasible in the less strained systems as the casa likely resulting from the cyano→acyl replacement).

σ– and π–Dimerizations of 1+2. The formation of σ–dimers of **1** (not in **2**) and of π–dimers of **2** (not in **1**), besides their chemical similarity, gives good account of the delicate balance of forces intervening in these dimerizations. Given that **1** and **2** form independently dimers, the question arises: would they form **1-2** σ–mixed dimers or alternatively **1-2** π–mixed dimers?

Figure 1f shows the UV-Vis absorption spectra of an equimolar dilute mixture of **1** and **2** by lowering the temperature (Figure S21). We detect two regimes: i) from 250 to 190 K where the intensities of the **1** and **2** monomer bands decrease allowing the development of two new bands at 274 nm and at 287 nm. These

values are on the range of those described in **σ-(1_2)** (277 and 286 nm) but slightly different which reveals the formation of a new species possibly of a mixed σ–dimer, or **σ-(1+2)**. ii) at 190 K, **σ-(1+2)** is seemingly unstable and its spectrum spontaneously evolves with time into a broad band at 577 nm, in the range of π–dimers, but again slightly different from that assigned in **π-(2_2)** (570 nm) which is therefore attributed to a new π–dimer, or **π-(1+2)**. TDDFT excited-state calculations in Table 1 further corroborate the formation of these **σ-(1+2)** and **π-(1+2)** mixed dimers.

Pressure induced dimerization/polymerization of 1. The Raman spectrum of the blue monomer of **1** in the solid in Figure 4 is typical of a quinononoid structure with strong bands around 1407 cm^{-1} due to the quinoidal thiophene C=C stretching modes, ν(C=C).[35,]

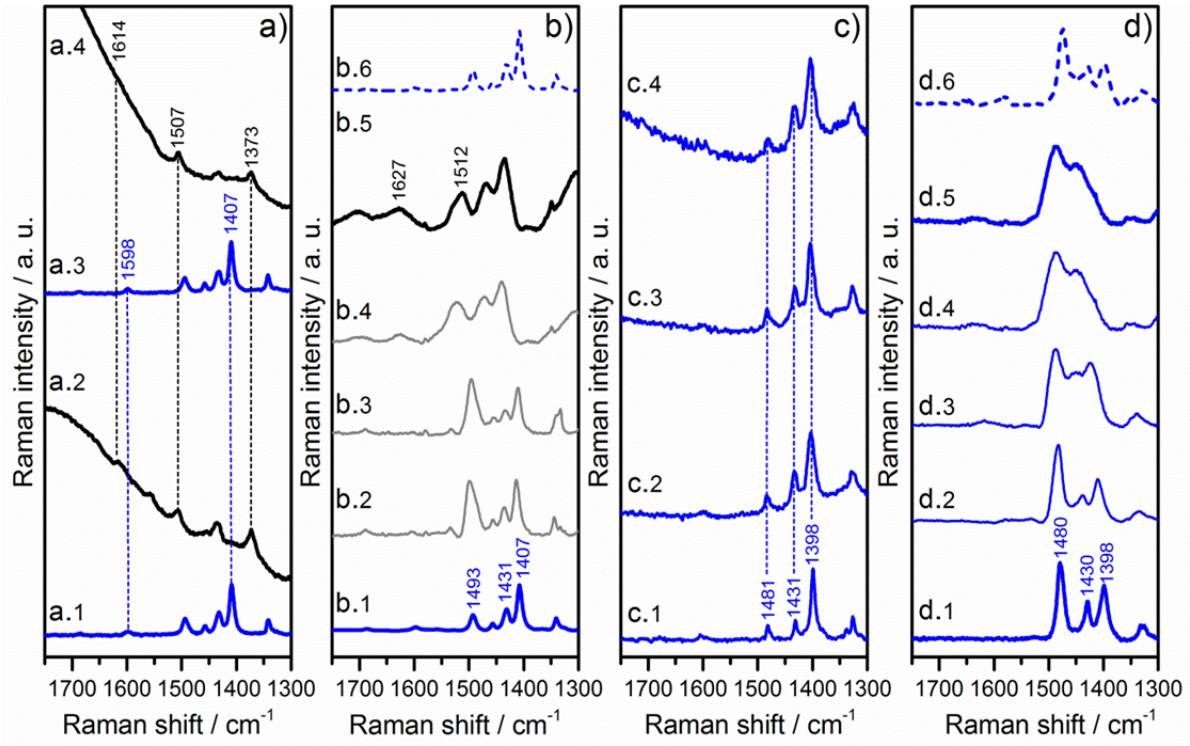

Figure 4 | Raman spectra of 1 and 2 at room temperature. a) Powder blue quinonoidal monomer **1** (a.1), colorless drop-cast thin film from solution (a.2), the above thin film heated at 400 K (a.3), re-dissolved and re-deposited as a drop-cast film (a.4). b) Powder blue quinoidal monomer **1** (b.1), 1 GPa (b.2), 3 GPa (b.3), 5 GPa (b.4), 6 GPa (b.5), pressure release (b.6). c) The same as (a) for compound **2**. d) The same as (b) for compound **2**. Raman spectra in (a) and (c) are taken with the 532 nm Raman excitation and those in (b) and (d) with the 785 nm Raman excitation.

In the colorless drop-cast thin solid film, the Raman spectrum completely changes and new bands at 1507/1614 cm^{-1} appear which are typical of ν(C=C) from aromatic thiophenes and naphthalene, respectively, emerging from the σ–polymer already described. This interpretation is strongly supported by the computed Raman spectra, Figure S22. **1** blue monomer under pressure at ≈ 6 GPa showed new Raman bands at 1510/20-1620 cm^{-1} similarly to those of the drop-cast σ–polymer whereas the original spectrum of **1** is fully recovered on pressure release. Under mechanical stress neighboring molecules of **1** are pushed closer promoting the generation of the radicaloid **σ-(1_2)-op** intermediate which could initiate a solid state polymerization resulting in an analogous backbone aromatic σ-polymer responsible of the Raman spectrum detected under pressure.

In summary, we have reported the chemically reversible formation of σ–dimers and σ– polymers in solution and in the solid state starting from a stable quinonoidal molecule. The dimerization/polymerization reaction provokes a shift of more than 2.5 eV of the electronic absorption bands from the monomer reactant to the σ–dimer/σ–polymer product. The reaction is reversible as a function of thermal, concentration and pressure cycling. Depending on the electron acceptor strength, these quinoidal naphthodithiophenes are able to form a variety of dimers: **σ-(1_2)** in the case of the cyanoester derivative, **π-(2_2)** for the dicyano case and, unexpectedly, both types for the mixed dimers, **σ-(1+2)** and **π-(1+2)**. This diversity of aggregation modes relies on the properties of the monomers providing two colors of the *two* structural "antagonistic" faces of the quinonoidal-*vs*-aromatic transformation (Janus-type molecules). Thus varying the chemical structure of the diradicaloid cores we are able to describe a novel reaction to prepare "reversible-made" chromic dimers and polymers and propose a mechanism that helps to understand fundamental properties of diverse aggregation modes of π–conjugated molecules. These soft materials can be envisaged for material applications utilizing the observed giant changes of the optical properties.

Methods. Palladium-catalyzed Takahashi reaction using the 2,7-dibromo-5,10-dialkyl-NDTs yields compound **1** similar to the syntheses of other thienoquinoidal molecules reported. Absorption spectra were recorded with a Cary 5000 spectrophotometer from Varian operating in a maximal 175–3300 nm range. UV-Vis-NIR spectra at different temperatures were carried out in an OPTISTAT cryostat from Oxford instruments. ^{1}H NMR data were obtained in a JEOL JNM-ECS400 spectrometer operating at 400 MHz for ^{1}H or 100 MHz for ^{13}C with tetramethylsilane (TMS) as an internal reference. All geometry optimizations were done at the (U)M05-2X/6-31G(d,p) level of theory using Gaussian 09.[36] All local minima were confirmed with all frequencies being real. Excited state time-dependent DFT (TDDFT) [33] calculations used 50 states and the same level of theory as the geometry optimizations. Solvent effects were considered by the polarizable continuum model (PCM).[37]

References.

[1] *Handbook of Conducting Polymers*, Third Edition, Edited by *Skotheim, T. A., Reynolds, J.*(CRC Press, USA, 2007).

[2] Kraft, A., Grimsdale, A., & Holmes, A. Electroluminescent Conjugated Polymers. Seeing Polymers in a new Light, *Angew. Chem. Int. Ed.* **47**, 402–428 (1998).

[3] Hoboken, N.J., *Principles of Polymerization, 4th Edition*, Edited by *Odian, G*. (Wiley, 2004).

[4] Functional Materials: Preparation, Processing and Applications *Edited by: S. Banerjee and A. Tyagi*, Elsevier Inc., 2012.

[5] Sonmez, G. & Wudl, F. Completion of the three primary colours: The final step toward plastic displays. *J. Mater. Chem.* **15**, 20–22 (2005).

[6] Bamfield, P., *Chromic Phenomena; technological applications of colour chemistry* (Royal Society of Chemistry, 2010).

[7]Jenekhe, S. A. & Kiserow, D. J. *Chromogenic Phenomena in Polymers* (American Chemical Society, 2004).

[8] Beaujuge, P. M. Ellinger, S. & Reynolds, J. R. The donor–acceptor approach allows a black-to-transmissive switching polymeric electrochrome. *Nat. Mater.* **7**, 795–799 (2008).

[9] Hatano, S. *et al.* Unusual Negative Photochromism via a Short-Lived Imidazolyl Radical of 1,1'-Binaphthyl-Bridged Imidazole Dimer. *J. Am. Chem. Soc*. **135**, 3164–3172 (2013).
[10] a) Goto, K. *et al.* A Stable Neutral Hydrocarbon Radical: Synthesis, Crystal Structure, and Physical Properties of 2,5,8-Tri-*tert*-butyl-phenalenyl, *J. Am. Chem. Soc*. **121**, 1619–1620 (1999). b) Lü, J. M. Rosokha, S. V., & Kochi, J. K. Stable (long bonded) dimers via de quantitative self-association of different cationic, anionic, and uncharged π-radicals: structures, energetic and optical transitions. *J. Am. Chem. Soc*. **125**, 12161–12171 (2003).
[11] Rudebusch, G. E. et al. Diindeno-fusion of an anthracene as a design strategy for stable organic biradicals. *Nat. Chem.* **2016**, DOI: 10.1038/nchem.2518.
[12] (a) Kubo, T. *et al*. Synthesis, Intermolecular Interaction, and Semiconductive Behavior of a Delocalized Singlet Biradical Hydrocarbon. *Angew. Chem. Int. Ed.* **44**, 6564 (2005). (b) Huang, J. & Kertesz, M. Intermolecular Covalent π−π Bonding Interaction Indicated by Bond Distances, Energy Bands, and Magnetism in Biphenalenyl Biradicaloid Molecular Crystal. *J. Am. Chem. Soc*. **129**, 1634-1643 (2007).
[13] Suzuki, S. *et al*. Aromaticity on the Pancake-Bonded Dimer of Neutral Phenalenyl Radical as Studied by MS and NMR Spectroscopies and NICS Analysis. *J. Am. Chem. Soc*. **128**, 2530–2531 (2006).
[14] Kikuchi, A. Iwahori, F.& J. Abe, Definitive Evidence for the Contribution of Biradical Character in a Closed-Shell Molecule, Derivative of 1,4-Bis-(4,5-diphenylimidazol-2-ylidene)cyclohexa-2,5-diene, *J. Am. Chem. Soc.* **126**, 6526–6527 (2004).
[15] Morita, Y. *et al*. Thermochromism in an organic crystal based on the co-existence of σ- and π-dimers. *Nat. Mater.* **7**, 48-51 (2008).
[16] Shimizu, A. et al. Resonance balance shift in stacks of delocalized singlet biradicals. *Angew. Chem. Int. Ed*. 48, 5482–5486 (2009).
[17] Cui, Z.-H. Lischka, H. Beneberu, H.Z. & Kertesz, M. Double Pancake Bonds: pushing the limits of strong π-π interactions, *J. Am. Chem. Soc*. **136**, 12958–12965 (2014).
[18] Mou, Z. Uchida, K. Kubo, T. & Kertesz, M. Evidence of σ– and π–dimerization in a series of phenalenyls, *J. Am. Chem. Soc.* **136**, 18009–18022 (2014).
[19] Takahashi, T. Matsuoka, K. Takimiya, K. Otsubo, & T. Aso, Y. Extensive Quinoidal Oligothiophenes with Dicyanomethylene Groups at Terminal Positions as Highly Amphoteric Redox Molecules, *J. Am. Chem. Soc.* **127**, 8928–8929 (2005).
[20] Ortiz, P.R. *et al.* On the Biradicaloid Nature of Long Quinoidal Oligothiophenes: Experimental Evidence Guided by Theoretical Studies. *Angew. Chem. Int. Ed*. **47**, 9057–9061 (2007).
[21] Quinoidal oligothiophenes: new properties behind an unconventional electronic structure, J. Casado, R.Ponce Ortiz, J. T. López Navarrete, *Chem. Soc. Rev.* , **41**, 5672–5686 (2012).
[22] Zeng, Z. *et al.* Pushing Extended *p*-Quinodimethanes to the Limit: Stable Tetracyano-oligo(*N*-annulated perylene)quinodimethanes with Tunable Ground States. *J. Am. Chem. Soc.* ***135***, 6363–6371 (2013).
[23] Morita, Y. Suzuki, S. Sato, K. Takui, T. Synthetic organic spin chemistry for structurally well-defined open-shell grapheme fragments, *Nat. Chem*. **3**, 197–204 (2011).
[24] Casado, J. *et al*. Quinoid Oligothiophenes as Electron-Donor and Electron-Acceptor Materials. A Spectroelectrochemical and Theoretical Study. *J. Am. Chem. Soc.* **124,** 12380–12388 (2002).
[25] Minami, T. & Nakano, M. Diradical Character View of Singlet Fission, *J. Phys. Chem. Lett.* **3**, 145–150 (2012).

[26] Varnavski, O. et al. High Yield Ultrafast Intramolecular Singlet Exciton Fission in a Quinoidal Bithiophene. *J. Phys. Chem. Lett.* **6**, 1375–1384 (2015).
[27] Mori, T. Yanai, N. Osaka, I. & Takimiya, K. Quinoidal Naphtho[1,2-*b*:5,6-*b*′]dithiophenes for Solution-Processed n-Channel Organic Field-Effect Transistors, *Org. Lett.* **16**, 1334–1337 (2014).
[28] Suzuki, Y. Miyazaki, E. & Takimiya, K. ((Alkyloxy)carbonyl)cyanomethylene-Substituted Thienoquinoidal Compounds: a New Class of Soluble n-Channel Organic Semiconductors for Air-Stable Organic Field-Effect Transistors, *J. Am. Chem. Soc.* **132**, 10453–10466 (2010).
[29] Parr, R. G. & Yang, W. *Density-functional theory of atoms and molecules* (Oxford Univ. Press, 1989).
[30] Zhao,Y. & Truhlar. D.G. The M06 suite of density functionals for main group thermochemistry, thermochemical kinetics, noncovalent interactions, excited states, and transition elements: two new functionals and systematic testing of four M06-class functionals and 12 other functionals. *Theor Chem Account*. **120**, 215–241 (2008).
[31] Petersson, G. A. Bennett, A. Tensfeldt, T. G. Al-Laham, M. A. Shirley, W. A. & Mantzaris, J. A complete basis set model chemistry. I. The total energies of closed-shell atoms and hydrides of the first-row atoms. *J. Chem. Phys*. **89** 2193–218 (1988).
[32] A few extremely stretched long CC bonds above 1.7 Å have been reported, see e.g. Toda, F. Tanaka, K. Stein, Z. & Goldberg, I. Extremely Long C-C Bonds in Strained 1,1,2,2-Tetraphenylcyclobutaarenes: 3,8-Dichloro-1,1,2,2-tetraphenyl-cyclobuta[*b*]naphthalene, $C_{36}H_{24}Cl_2$, and 3,6,9,10-Tetrachloro-4,5-dimethyl-1,1,2,2,7,7,8,8-octaphenyldicyclobuta[b,h]phenanthrene Toluene Solvate, $C_{68}H_{46}Cl_4.1.5C_7H_8$. *Acta Crystallogr., Sect. C* **52**, 177(1996).
[33] Bauernschmitt, R. & Ahlrichs, R. Treatment of electronic excitations within the adiabatic approximation of time dependent density functional theory. *Chem. Phys. Lett*. **256**, 454–464 (1996).
[34] The EPR analysis provides more evidences if a more concentrated solution than 3mg/mL is studied. Its EPR signal consists of a doublet assigned to the hyperfine couplings of the diradical only with the thiophene and naphthalene H atoms (not with the N atoms, see supporting information). We can attribute this to the concurrent $sp^2 \rightarrow sp^3$ pyramidalization of the carbon atoms that form the long CC bonds during polymerization which decouples the π-electron density of the external cyano groups from the central core. When the temperature is lowered, the localization of the electron density in the -CN groups leads to a fast polymerization (since the solution is very concentrated), precluding the observation of the corresponding hyperfine coupling with the N atom.
[35] Hernández, V., et al., Vibrational spectroscopic study of 5,5′′′-bis(dicyanomethylene)5,5″-bis(dicyanomethylene)-5,5′′′-dihydro-Δ2,2′:5′,2′′′-5,5″-dihydro-Δ2,2′:5′,2″-terthiophene bearing a heteroquinonoid structure as a model of doped polythiophene, *J. Chem. Phys.* **109**, 2543–2548 (1998)
[36] Gaussian 09, Revision A.02, Frisch, M. J. *et al.* Gaussian, Inc., Wallingford CT, **2009**.
[37] Tomasi, J. Mennucci, B. & Cammi, R. Quantum Mechanical Continuum Solvation Models. *Chem. Rev*. **105**, 2999–3093 (2005).

Acknowledgments

We thank MINECO of Spain Government (CTQ2012-33733,), Junta de Andalucía (P09-FQM-4708) and Generalitat Valenciana (Prometeo-II2014/076 and ISIC projects) for the financial support of the work at the Universities of Málaga and Valencia. JLZ thanks the Research Central Services (SCAI) of the University of Málaga. This work was financially supported by JSPS KAKENHI Grant Numbers 23245041 and 15H02196 and by ImPACT Program of Council for Science, Technology and Innovation (Cabinet Office, Government of Japan). We thank the U.S. National Science Foundation for its support of this research at Georgetown University (grant no. CHE-1006702). M.K. is member of the Georgetown Institute of Soft Matter.

Author contributions

J.C. and K.T. designed the project. J.L.Z. carried out the optical characterization of the reactions. N.Y., T.M. and M.N. performed the synthesis of **1** and data analysis. L.Q. and M.K. carried out quantum chemical calculations. C.J.G.G. carried out the EPR and magnetic susceptibility characterization. J.C., K.T., J.T.L.N. and M.K. wrote the manuscript.

Additional information

Supplementary information is available in the online version of the paper. Reprints and permissions information is available online at www.nature.com/reprints. Correspondence and requests for materials should be addressed to K.T. or J.C.

Competing financial interests

The authors declare no competing financial interests.